

Probing antiferromagnetism in NiMn/Ni/(Co)/Cu₃Au(001) single-crystalline epitaxial thin films

M. Yaqoob Khan, Chii-Bin Wu, Mustafa Erkovan, and Wolfgang Kuch

Citation: *Journal of Applied Physics* **113**, 023913 (2013); doi: 10.1063/1.4775575

View online: <http://dx.doi.org/10.1063/1.4775575>

View Table of Contents: <http://scitation.aip.org/content/aip/journal/jap/113/2?ver=pdfcov>

Published by the **AIP Publishing**



Goodfellow

metals • ceramics • polymers
composites • compounds • glasses

Save 5% • Buy online
70,000 products • Fast shipping

Probing antiferromagnetism in NiMn/Ni/(Co)/Cu₃Au(001) single-crystalline epitaxial thin films

M. Yaqoob Khan,^{a)} Chii-Bin Wu (吳啟彬), Mustafa Erkovan,^{b)} and Wolfgang Kuch
Institut für Experimentalphysik, Freie Universität Berlin, 14195 Berlin, Germany

(Received 9 November 2012; accepted 20 December 2012; published online 14 January 2013)

Antiferromagnetism of equi-atomic single-crystalline NiMn thin film alloys grown on Ni/Cu₃Au(001) is probed by means of magneto-optical Kerr effect (MOKE). Thickness-dependent coercivity (H_C) enhancement of polar MOKE measurements in NiMn/Ni/Cu₃Au(001) shows that ~ 7 atomic monolayers (MLs) NiMn order antiferromagnetically at room temperature. It is found that NiMn can couple to out-of-plane (OoP) as well as in-plane (IP) magnetized Ni films, the latter stabilized by Co under-layer deposition. The antiferromagnetic (AFM) ordering temperature (T_{AFM}) of NiMn coupled to OoP Ni is found to be much higher (up to 110 K difference) than in the IP case, for similar interfacial conditions. This is attributed to a magnetic proximity effect in which the ferromagnetic (FM) layer substantially influences T_{AFM} of the adjacent AFM layer, and can be explained by either (i) a higher interfacial coupling strength and/or (ii) a thermally more stable NiMn spin structure when coupled to Ni magnetized in OoP direction than in IP. An exchange-bias effect could only be observed for the thickest NiMn film studied (35.7 ML); the exchange-bias field is higher in the OoP exchange-coupled system than in the IP one, possibly due to the same reason/s. © 2013 American Institute of Physics. [<http://dx.doi.org/10.1063/1.4775575>]

I. INTRODUCTION

Antiferromagnetic (AFM) thin films are basic components of spintronic devices¹ which depend on the exchange-bias (EB) effect discovered more than half a century ago.² An AFM layer provides a reference magnetization direction to the ferromagnetic (FM) layer in these kinds of magneto-electronic devices, e.g., hard-disk read heads,³ or magnetic random-access memories.⁴ In the EB effect an FM and an AFM material couple to each other, mostly by direct exchange interaction, whereby not only the coercivity of the FM is enhanced, but the hysteresis loop is also shifted along the magnetic field axis below a certain blocking temperature.^{2,5} Although it is accepted that for EB the spin-spin interaction at the FM-AFM interface is necessary, EB is influenced by several effects like interface roughness, crystalline and magnetic structure, chemical order, composition, or magnetic proximity effects. Therefore the behaviour of the EB effect varies from system to system and from material to material, and hence it is often stated that despite its high technological importance and the tremendous amount of work done on this subject, EB is not yet generally well understood.

Among the antiferromagnetic materials, Mn-based alloys having a face-centered-tetragonal crystalline structure provide very high blocking temperatures, good corrosion resistance, and high exchange-bias field, and thus are very suitable to be used in real devices.⁶ The major drawback of these materials is their large critical thickness which could limit their application in ultra-high density recording applications.⁶ NiMn plays a leading role in these materials,

having the highest antiferromagnetic ordering temperature (T_{AFM}) amongst all Mn-based alloys (as high as 1070 K in the bulk)^{7,8} and, if prepared bulk-like in single-crystalline form, might maintain such a high ordering temperature suitable to be used at elevated temperatures in practical devices.

The motivation for probing the antiferromagnetism of NiMn on top of Ni/(Co)/Cu₃Au(001) is two-fold. First, it is interesting to see which spin structure NiMn exhibits in thin films on Cu₃Au(001), where it grows with bulk-like lattice parameters.⁹ Epitaxial FeMn on Cu(001) has proven to couple to both IP and OoP magnetized FM layers^{10,11} and shows a non-collinear spin structure.^{12,13} Different from our previous work,⁹ where in the studied regime of thickness, concentration, and temperature we could not see any coupling of NiMn to an IP-magnetized Co layer in the system Co/Ni_xMn_{1-x}/Cu₃Au(001), we wanted to use Ni as the ferromagnetic material because its easy axis can be tuned to be either along the OoP or the IP direction. In thin film form, NiMn may not have the same collinear spin structure as reported for its bulk form.^{14,15} In the bulk AF I-type spin structure of $L1_0$ NiMn, the nearest-neighbor Mn atom's moments are antiparallely aligned and oriented normal to the c -axis of the fct lattice. The Mn and Ni atoms constitute alternating sheets with magnetic moments of $3.8 \mu_B$ and approximately $0 \mu_B$ per atom, respectively.^{14,16,17} The second motivation is the high Néel temperature of NiMn: Ni₅₀Mn₅₀/Cu₃Au(001) can be prepared epitaxially along its c -axis in single-crystalline form like that of its bulk counterpart,⁹ and may thus have a very high T_{AFM} . Furthermore, since EB is an interface phenomenon, its investigation can be more appropriately addressed using single-crystalline materials than polycrystalline ones.

Like other Mn-based alloys, NiMn has been mostly studied in its polycrystalline form prepared by magnetron

^{a)}Present address: Kohat University of Science and Technology, Kohat 26000, Khyber Pukhtunkhwa, Pakistan.

^{b)}Present address: Department of Physics, Gebze Institute of Technology, P.K. 141, 41400 Gebze-Kocaeli, Turkey.

sputtering. No study of single-crystalline NiMn thin films has been reported until the last few years. For epitaxially grown NiMn thin films, studies have been recently performed on Cu(111),¹⁸ Cu(001),^{19–21} and Cu₃Au(001)⁹ as substrates. Ni/NiMn/Cu(111) needed annealing in the presence of a magnetic field and then showed a complex temperature-dependent exchange bias for a thickness of 35 Å.¹⁸ Tieg *et al.* showed antiferromagnetism of equi-atomic NiMn in the bilayer system Co/NiMn/(Co)/Cu(001), where NiMn grows with its *a*-axis along the surface normal.¹⁹ The enhancement of coercivity of Co was attributed to the interface magnetic coupling due to the antiferromagnetic character of NiMn above 8 ML thickness at 300 K.¹⁹ Reinhardt *et al.* not only confirmed these findings for a similar system afterwards, but also found stronger coupling in Co/Ni₃₅Mn₆₅/Cu(001) as compared to Co/Ni₅₀Mn₅₀/Cu(001).²⁰ Macedo *et al.* studied the system Co/NiMn/Cu₃Au(001), but could not observe any antiferromagnetic order up to the maximum studied thickness of 14.5 ML Ni₅₀Mn₅₀ down to a temperature of 190 K.⁹ Referring to Reinhardt *et al.*'s findings, Macedo *et al.* also searched for the evidence of FM/AFM coupling in Co/NiMn bilayers on Cu₃Au(100) for two Ni concentrations below the *L*₁₀ range, i.e., at Ni concentrations of 23% and 33%, but no coupling at the interface was observed.⁹ In a combined experimental and theoretical investigation, Gao *et al.* have shown by spin-polarized scanning tunneling microscopy that the surface spin density of NiMn/Cu(001) films is non-collinear,²¹ contrary to what was expected. This was assigned to the broken symmetry at the surface.²¹ According to our information, the magnetic properties (like the antiferromagnetic ordering temperature T_{AFM} , the blocking temperature for exchange bias T_b , and the exchange bias field H_{eb}) of NiMn single-crystalline thin films have never been reported in contact to OoP magnetized FM layers on any substrate including Cu₃Au(001). For NiMn in contact to an IP magnetized FM layer, only a few thickness- and temperature-dependent magneto-optical Kerr effect (MOKE) measurements have been performed on Cu(001),^{19,20} limited to exploring T_{AFM} .

We present here a systematic comparative study of the magnetic properties of epitaxially grown equi-atomic 7.4–35.7 ML NiMn films when coupled to IP Ni/Co/Cu₃Au(001) and OoP Ni/Cu₃Au(001). NiMn/Ni/(Co)/Cu₃Au(001) was used rather than (Co)/Ni/NiMn/Cu₃Au(001), because in the latter case the spin reorientation transition (SRT) of Ni from OoP to IP magnetization (not shown here) refrained us from doing so. This SRT of the Ni overlayer is very sensitive to the Ni and NiMn thickness, NiMn composition, as well as temperature. To study the influence of the magnetization direction on the coupling between Ni and NiMn, on one half of the substrate spontaneously OoP magnetized 12–13 ML Ni is used. On the other half, Ni of the same thickness is made IP by first depositing ~2 ML Co underneath. We find that the T_{AFM} of the very same NiMn film is much higher when it is coupled to OoP Ni than to IP Ni. For example, for the thinnest two films under study, i.e., of 7.4 and 11.3 ML thicknesses, this difference of T_{AFM} is 110 K. Our results resemble a previous finding for FeMn films in (Co)/Ni/FeMn/Cu(001), where this difference of T_{AFM} was up to

60 K for about 7–8 ML FeMn.¹⁰ In Ref. 10, this difference has been attributed to a magnetic proximity effect which is proposed to be due to higher coupling strength in the OoP direction than in IP. This supports results of Ref. 11 for FeMn, where indications for different FeMn critical thicknesses coupled to OoP and IP FM layers had been presented. Recently, Stampe *et al.*²² showed that the interface roughness and Fe concentration both contribute to the FM-AFM coupling strength in the OoP direction, but that T_{AFM} is independent of the coupling strength, while it shows a strong dependence on the FM magnetization direction. This points towards an effect induced by the AFM spin structure, which could be influenced by the interface coupling.

II. EXPERIMENTAL ASPECTS

All the experiments were performed under ultra-high vacuum conditions, and a pressure of $\sim 10^{-10}$ mbar could be maintained during the preparation of the sample. The chamber was equipped with Ar⁺ ion sputtering, annealing, e-beam evaporators, medium energy electron diffraction (MEED), low energy electron diffraction (LEED), Auger electron spectroscopy (AES), and MOKE in polar and longitudinal geometries. The sample was cleaned by Ar⁺ ions with an energy of 1 keV, and the cleanliness of the sample was then checked by AES. After sputtering and AES, the sample was annealed at 800 K for ~10 min to order the surface. A shutter was positioned as close as possible (~3 mm) in front of the prepared sample, covering the lower half, and ~2 ML Co were evaporated on the upper half. Previously, for a wedged Co sample, in the system Co/Ni/FeMn/Ni/Cu(001), it was shown by magnetic domain images that with a Co thickness of higher than 0.5 ML, the magnetization of 15 ML Ni changed from OoP to IP direction.¹¹ After removing the shutter, 12–13 ML Ni were evaporated on the entire sample which then have OoP magnetization at the lower half and IP magnetization at the upper half of the sample due to the underlying ~2 ML Co. At the lower half of the sample (without Co), the (00) MEED spot intensity versus time during evaporation was observed on a fluorescent screen opposite to the electron gun for a beam energy of 2 keV. The typical growth rate of Ni was 1 ML per minute and was monitored by MEED oscillations. At room temperature, the IP-to-OoP spin-reorientation transition (SRT) thickness of Ni/Cu₃Au(001) was found to be 8 ML, while the OoP-to-IP one was 17 ML. Immediately after Ni evaporation, Mn and Ni are co-evaporated to obtain an equi-atomic NiMn alloy of thicknesses ranging from 7.4 to 35.7 ML. By “equi-atomic,” we mean a Ni concentration between 45% and 55%. All the three materials used for evaporation were of high purity (Co and Ni: 99.99%, Mn: 99.95%). NiMn does not grow layer-by-layer on Ni/Cu₃Au(001), so its thickness cannot be directly inferred from MEED. Instead, AES was utilized to determine the concentration of NiMn. The thickness of NiMn can then be determined, since the evaporation rate of Ni was fixed to be the same for Ni and NiMn preparation. For the determination of NiMn thicknesses by AES below 15 ML, the contribution from the Ni underlayer had to be taken into account. All films were deposited at room temperature.

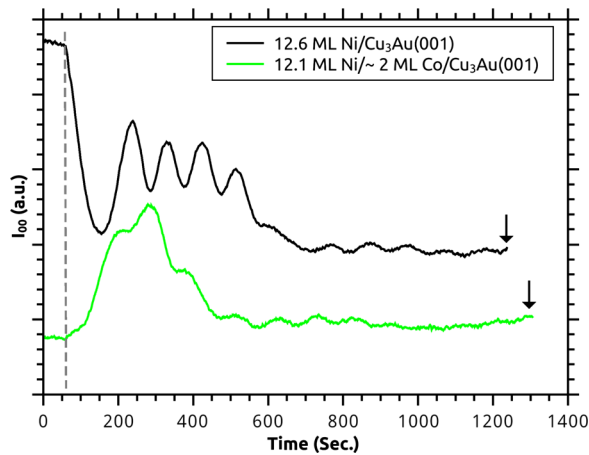


FIG. 1. MEED (00)-spot intensity recorded during the deposition of 12.6 ML Ni on $\text{Cu}_3\text{Au}(001)$ (upper curve), and 12.1 ML Ni on ~ 2 ML $\text{Co}/\text{Cu}_3\text{Au}(001)$ (lower curve) at $T = 300$ K. The dotted vertical line at 60 s shows the opening of the shutter and the down arrows at the end of the curves indicate the closing of the shutter.

To address the magnetic properties of $\text{NiMn}/\text{Ni}/(\text{Co})/\text{Cu}_3\text{Au}(001)$, we made use of longitudinal and polar MOKE geometries to study the IP and the OoP magnetization at the upper and the lower half of the sample, respectively. Linearly polarized laser light from a laser diode of 1 mW power and 635 nm wavelength was used. A field-cooling process was applied with the maximum available external magnetic field of ± 200 mT from a temperature of 480 K. The minimum attainable temperature for the MOKE measurements was ~ 140 K.

III. RESULTS

Since one purpose of the present study is the comparison of the magnetic properties of NiMn/Ni bilayers grown directly on $\text{Cu}_3\text{Au}(001)$ and on $\text{Co}/\text{Cu}_3\text{Au}(001)$, it is important to show that the surface roughness and crystalline structures of Ni on $\text{Cu}_3\text{Au}(001)$ and on $\text{Co}/\text{Cu}_3\text{Au}(001)$ are very similar. Fig. 1 presents, on the same scale, MEED intensity oscillations of the specular beam during growth of Ni on

$\text{Cu}_3\text{Au}(001)$ (black line) and on 2 ML $\text{Co}/\text{Cu}_3\text{Au}(001)$ (green line). The oscillation maxima indicate the deposition of successive atomic monolayers in a layer-by-layer growth mode. While on the clean $\text{Cu}_3\text{Au}(001)$ substrate the reflected electron intensity drops during the initial stages of Ni deposition, the intensity initially increases when Ni is deposited on $\text{Co}/\text{Cu}_3\text{Au}(001)$. This increase can be attributed to the filling of atomic-scale roughnesses at the Co surface by Ni. The subsequent intensity oscillations up to a thickness of about 6 ML are more pronounced in $\text{Ni}/\text{Cu}_3\text{Au}(001)$. At higher thicknesses, however, the two curves become very similar. We conclude that the morphology of the Ni surface, and thus of the NiMn/Ni interface, is very similar in the two systems once the Ni thickness exceeds about 6 ML.

Also, from Fig. 2(a), it is clear that the LEED patterns of 12.4 ML $\text{Ni}/\text{Cu}_3\text{Au}(001)$ and that of 12.4 ML $\text{Ni}/\sim 2$ ML $\text{Co}/\text{Cu}_3\text{Au}(001)$ are identical at similar energies. A linear fitting of the E_{kin} versus n^2 points extracted from the $I(V)$ curves (Fig. 2(b)) gives the vertical interlayer distance d_p . The straight lines in Fig. 2(b) represent linear fittings based on the kinematic approximation of the (00) diffraction beam intensity, and provide the perpendicular lattice constant of 14.7 ML $\text{Ni}/\text{Cu}_3\text{Au}(001)$ and that of 12.1 ML $\text{Ni}/\sim 2$ ML $\text{Co}/\text{Cu}_3\text{Au}(001)$. The exactly matching result $d_p = 1.74 \text{ \AA}$ indicates a very similar Ni structure for the two cases.

Figure 3 shows our results for the coercivity of OoP magnetized Ni films versus the thickness of equi-atomic NiMn in n ML $\text{NiMn}/9.3$ ML $\text{Ni}/\text{Cu}_3\text{Au}(001)$, where $\sim 7 \leq n \leq \sim 28$, measured at room temperature. A steady increase of the coercivity of OoP magnetized 9.3 ML $\text{Ni}/\text{Cu}_3\text{Au}(001)$ with NiMn thickness can be observed. With ~ 7 ML of NiMn , the bilayer has already a distinctly higher coercivity as compared to the Ni film alone. The inset of Fig. 3 shows as an example magnetization curves of 9.3 ML Ni without NiMn coverage (filled circles) and with ~ 28 ML NiMn (open-circles), the latter exhibiting a much higher coercivity, but no exchange bias at 300 K.

An example of temperature-dependent hysteresis loops for both OoP as well as IP magnetization is shown in Fig. 4. Here the sample is 11.3 ML $\text{NiMn}/12.5$ ML Ni with (Fig. 4(a))

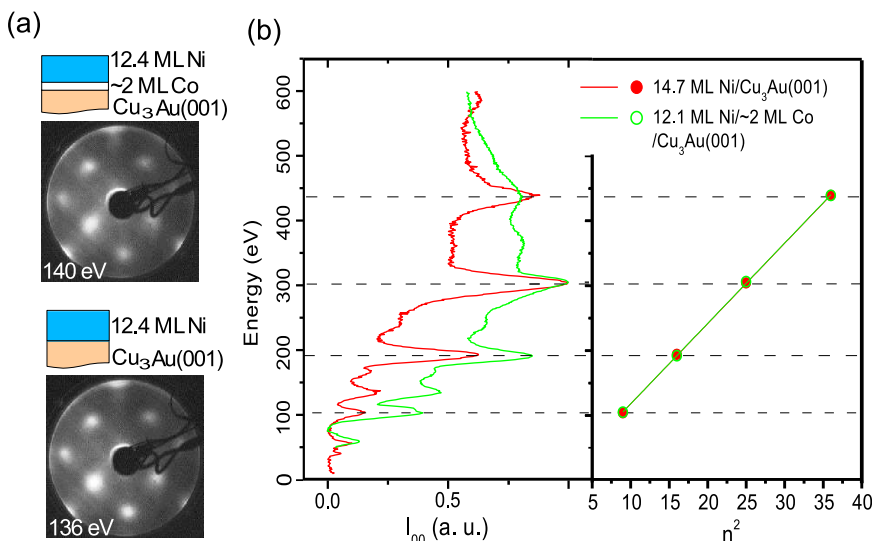


FIG. 2. LEED pattern ($p(1 \times 1)$ unit cell) of (a) 12.4 ML $\text{Ni}/\sim 2$ ML $\text{Co}/\text{Cu}_3\text{Au}(001)$ for 140 eV and that of 12.4 ML $\text{Ni}/\text{Cu}_3\text{Au}(001)$ for 136 eV. (b) LEED $I(V)$ curves for 14.7 ML $\text{Ni}/\text{Cu}_3\text{Au}(001)$ (red line) and 12.1 ML $\text{Ni}/\sim 2$ ML $\text{Co}/\text{Cu}_3\text{Au}(001)$ (green line), and peak energy dependence of LEED $I(V)$ curves on n^2 (n being Bragg diffraction order) for 14.7 ML $\text{Ni}/\text{Cu}_3\text{Au}(001)$ (red symbols) and 12.1 ML $\text{Ni}/\sim 2$ ML $\text{Co}/\text{Cu}_3\text{Au}(001)$ (green symbols). Note that data points in both cases overlap.

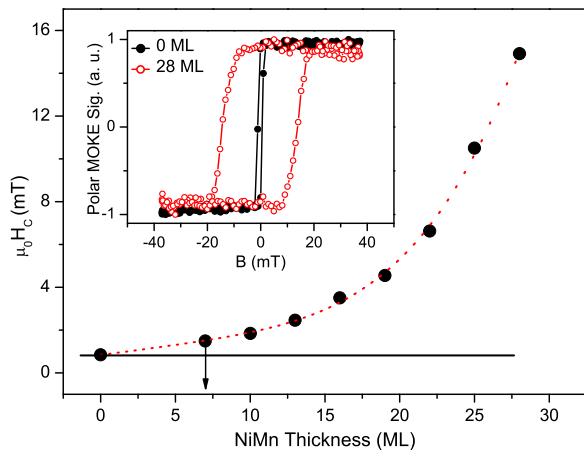


FIG. 3. Coercivity (H_C) versus NiMn thickness for the bilayer system NiMn/9.3 ML Ni/Cu₃ Au(001) measured by polar MOKE. The red-dotted line is a guide to the eye. The black horizontal line passing through the first point of the curve (0 ML NiMn/9.3 ML Ni) shows the deviation of H_C due to NiMn. In the inset the normalized Kerr intensity is shown for (i) uncovered 9.3 ML Ni/Cu₃ Au(001) (black loop with closed symbols) and (ii) the same film covered with ~ 28 ML NiMn (red loop with open symbols).

and without ~ 2 ML Co underneath (Fig. 4(b)), on Cu₃Au (001). Rectangularly shaped loops for both cases were obtained, where a coercivity enhancement with decreasing temperature can be observed. Although the general behaviour

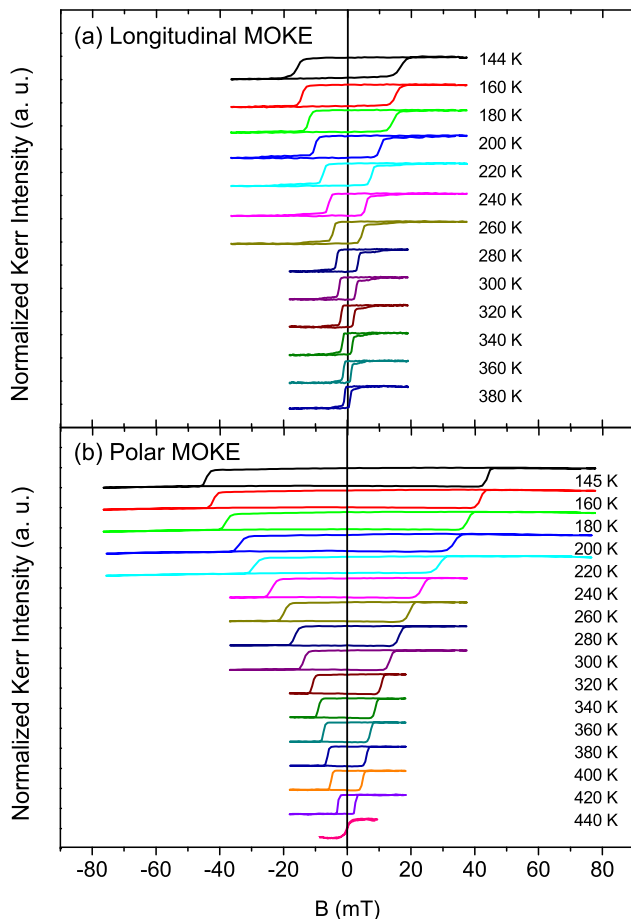


FIG. 4. Normalized magnetic hysteresis loops at different temperatures for (a) 11.3 ML NiMn/12.5 ML Ni/ ~ 2 ML Co/Cu₃Au(001) and (b) 11.3 ML NiMn/12.5 ML Ni/Cu₃Au(001) measured by longitudinal and polar MOKE, respectively.

of the temperature-dependent hysteresis loops is similar for the IP and OoP cases, the details are different (Fig. 4). The main differences between the two magnetization directions observed here are that the coercivity H_C for OoP magnetization is almost three times that for IP magnetization at low temperatures, and that the reduction of H_C to lower values occurs at higher temperatures for OoP magnetization of the Ni layer (loop at 440 K).

Fig. 5 shows the temperature-dependent coercivity for IP and OoP magnetized Ni films in contact to an n ML NiMn film ($\sim 7 \leq n \leq \sim 35$) on the positive field axes. The insets of Figs. 5(a) and 5(b) show a zoom-in of H_C versus temperature for 7.4 ML NiMn in contact with IP and OoP Ni, respectively. The purpose of these insets is to show how we determine the ordering temperature of AFM NiMn. If there were no exchange coupling between the AFM and the FM layers, the H_C of the FM layer alone would decrease monotonically as the temperature is increased, and would give rise to a certain slope of small steepness. We observe, in contrast, in Fig. 5(a) for all IP films a discontinuity in the slope of H_C versus temperature curves which is typical for AFM/FM bilayer exchanged-coupled systems.^{10,22,23} The point at which this discontinuity of temperature-dependent H_C occurs is considered as T_{AFM} . For its determination, we follow the procedure already used in Ref. 22, and fit a straight line to the $H_C(T)$

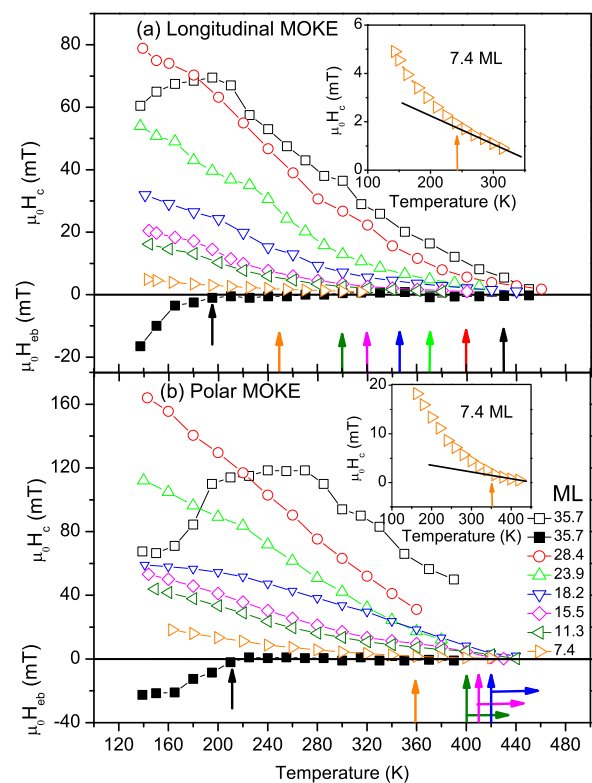


FIG. 5. Temperature dependence of the coercivity (positive field axis) and the exchange-bias field (negative field axis) for different thicknesses of NiMn grown on (a) in-plane-magnetized ~ 12 ML Ni/ ~ 2 ML Co/Cu₃Au (001) and (b) out-of-plane magnetized ~ 12 ML Ni/Cu₃Au(001). In the respective insets, a zoom-in on the curve for 7.4 ML NiMn is presented to show how the antiferromagnetic ordering temperature is determined. The obtained antiferromagnetic ordering temperatures are indicated by colored arrows, where the horizontal bars at 11.3, 15.5, and 18.2 ML NiMn in (b) denote that they just represent lower limits.

data in the high-temperature range to represent the behavior of the uncoupled FM layer. The temperature at which the measured H_C significantly deviates from this line is defined as T_{AFM} , and marked by colored arrows in Fig. 5. For the OoP magnetized Ni, this kind of discontinuity could only be seen for the thinnest (7.4 ML) studied NiMn film. For the thicker films up to 18 ML thickness, only lower limits for T_{AFM} can be given, indicated by horizontal arrows next to the vertical arrows in Fig. 5(b). For the three thickest NiMn films, it was not possible to get any information on T_{AFM} , since an easy-axis change of the Ni magnetization from OoP to IP occurs at a temperature lower than the ordering temperature.

From Fig. 5(a), one can see that for the IP samples the T_{AFM} value initially increases by 30 to 40 K every 3 to 4 ML of NiMn thickness. For the OoP part, a similar increment of T_{AFM} is observed when increasing the NiMn thickness from 7.4 to 11.3 ML. This increase of T_{AFM} with increasing AFM layer thickness is due to the well-known finite-size effect and is in agreement with results for FeMn/Co/Cu(001)²³ and (Co)/Ni/FeMn/Cu(001)¹⁰ for both, the IP and OoP cases. Like in Refs. 10 and 11 for FeMn, we also found that the critical thickness of the NiMn films to form antiferromagnetic order at room temperature (300 K) varies with changing the magnetization direction of the FM layer from OoP to IP. Comparing the exchange-coupled AFM/FM samples shown in Figs. 5(a) and 5(b), one observes that the ordering temperature of the same NiMn thickness is distinctly higher for the OoP coupled part than for the IP one. This difference is 110 K for the thinnest film with 7.4 ML thickness.

The exchange coupling in the NiMn/Ni/(Co)/Cu₃Au(001) system also resulted in shifted loops with an exchange-bias field (H_{eb}), but only at the thickest (35.7 ML) studied NiMn film as shown in Figs. 5(a) and 5(b) by black solid symbols on the negative side of the vertical axes for IP as well as OoP magnetized Ni, respectively. A common feature for both the IP and OoP exchange-biased systems is that the coercivity goes down with lower temperature as soon as exchange bias is established. This behavior has been observed for several other systems.^{24–27} Both, the H_{eb} value and the blocking temperature T_b , the latter indicated by black arrows in Fig. 5, are slightly higher in the case of NiMn coupled to OoP Ni than in the IP case. The ratio of the exchange-bias field to the coercivity, however, is smaller for OoP compared to IP.

IV. DISCUSSION

In Ref. 9, no influence of a NiMn layer with thickness up to 14.5 ML on the magnetic properties of a FM Co layer in Co/NiMn/Cu₃Au(001) was observed because of either chemical and/or crystallographic disorder, or because the NiMn spin order was perpendicular to the Co magnetization. We will discuss the latter argument first. In FM/AFM bilayer systems, if the FM film thickness is kept constant, its coercivity increases with increasing thickness of the AFM thin film above the critical thickness for the onset of antiferromagnetic order. We observed this enhancement of coercivity in our bilayer system and found that its critical thickness is

less than ~ 7 ML for the OoP sample at room temperature. This critical thickness is smaller than the one of 8 ML reported for NiMn/6 ML Co/Cu(001).^{19,20} This could be due to the fact that the reported measurements have been done on an IP system whereas we performed it for the OoP one. Our result is similar to the observations in the system (Co)/Ni/FeMn/Cu(001), where the critical thickness is smaller for the case when the adjacent Ni is magnetized in the OoP direction than in IP.^{10,11}

As mentioned in the introduction, one of the objectives of the present study was to check whether the spin structure of epitaxially grown NiMn thin films deviates from a simple collinear spin structure. The observed coupling of the NiMn layer to both IP and OoP magnetized adjacent FM layers (Figs. 4 and 5) is either a hint towards a non-collinear spin structure or it shows that the NiMn spins can be tilted in either direction. Comparing the IP versus OoP samples for otherwise identical conditions, the striking difference is the T_{AFM} . The T_{AFM} for the OoP samples is as much as 110 K higher than for the IP samples. This can be attributed to the magnetic proximity effect in which the proximity of the magnetized FM layer raises the T_{AFM} of the AFM layer. The significance of this effect is that just by changing the magnetization direction of the adjacent FM layer, the very same NiMn film could be switched from the antiferromagnetic state to the paramagnetic one and vice versa. Our findings are similar to the ones reported for FeMn,¹⁰ where up to 60 K decrease of T_{AFM} is observed when the OoP Ni magnetization is switched to IP by deposition of a Co over-layer in the system (Co)/Ni/FeMn/Cu(001). The reason for the magnetic proximity effect leading to this difference in T_{AFM} has been related to the well-known three-dimensional bulk-like spin structure of FeMn.^{12,13} This strengthens our assumption about a three-dimensional spin structure of NiMn on Cu₃Au(001).

This magnetic proximity effect could be due to either a different coupling strength at the AFM/FM interface in the IP and the OoP direction and/or a different interfacial spin structure of NiMn. If a 3*Q*-like three-dimensional spin structure of NiMn is assumed, a higher coupling strength in the OoP direction compared to IP could be one possible reason for the higher T_{AFM} . This higher coupling strength in the OoP direction could be justified under the assumption of large terraces of NiMn at the interface, as has been assumed for FeMn.¹⁰ Assuming 3*Q*-like spin structure, the IP component of the NiMn surface spins in one terrace should cancel each other, but not the OoP component. In the IP direction, uncompensated spins contribute only from the step edges,²⁸ where their density would be smaller compared to OoP uncompensated spins at large terraces. Therefore, the OoP uncompensated spins on the large terraces would lead to a higher coupling strength and hence a higher T_{AFM} as compared to the coupling strength from IP uncompensated spins at step edges. Recently, Stampe *et al.*²² have reported that for OoP magnetization in FeMn/Ni/Cu(001), the interfacial coupling strength does not influence the T_{AFM} of FeMn. We do not exclude the contribution of the coupling strength towards the T_{AFM} of NiMn here. In the NiMn/Ni/(Co)/Cu₃Au(001) system, we did not vary the AFM/FM interfacial

coupling strength independently from the direction of easy axis of the FM, we therefore cannot conclude whether in our system the coupling strength has a direct influence on T_{AFM} . But, besides the difference in the lattice structural properties, the magnetic properties of both FeMn and NiMn might also be different. One considerable difference is that the Fe magnetic moment is comparable to that of Mn in FeMn, whereas in NiMn, the Ni magnetic moment is negligibly small as compared to the Mn moment.^{14,16,17} Therefore, in spite of possibly having a similar spin structure, the coupling strength may have a different effect on T_{AFM} in both materials, such that we cannot exclude the possibility that it could play a role. An alternative mechanism, not relying on the coupling strength, has been proposed to explain the different T_{AFM} when the adjacent FM layer magnetization is switched from OoP to IP²²—the $3Q$ spin structure of the AFM layer could be differently distorted when coupled to an FM layer in IP and OoP direction. A different spin structure can result in different T_{AFM} if the average exchange coupling between the antiferromagnetic spins in the AFM layer depends on their relative orientations. In the assumed $3Q$ -like spin structure of NiMn, the OoP AFM/FM coupling may lead to the rearrangement of NiMn spins towards a $1Q$ -like OoP spin structure at and near the interface. The opposite situation may occur for the IP case, where the NiMn spins are rearranged towards a $2Q$ -like IP spin structure. If the spin structure in the OoP coupling were more thermally stable than the IP one, this could give rise to a higher T_{AFM} in the former case.

When we compare our results to Refs. 10, 11, and 22, we can speculate that the spin structure of our studied NiMn films at the interface is either non-collinear, contrary to the reported collinear spin structure of bulk NiMn,^{14,15} or that the spins of the NiMn layer acquire the respective directions of the adjacent FM Ni layer after the field cooling process. As a result, the NiMn spin structure could be thermally more stable when coupled to OoP Ni than to IP.

In the light of our speculations about the mechanism for having different T_{AFM} of NiMn coupled to Ni magnetized along different axes, one can further speculate about the reason for the absence of any apparent coupling of 12 ML Co in contact with 14.5 ML NiMn/Cu₃Au(001), even at 190 K, as reported in Ref. 9. A smaller coupling strength and/or differently distorted $3Q$ -like spin structure of NiMn in contact to Co might result in a smaller T_{AFM} below the measured temperature range. Furthermore, the larger magnetization of Co, as compared to Ni, would certainly result in a reduced coercivity.

We could only find exchange bias in the thickest NiMn film studied (35.7 ML), together with a peak in coercivity near T_b . The blocking temperature and exchange-bias field are also higher for the OoP case than for IP. This could be directly related to the higher antiferromagnetic ordering temperature in the former case. At temperatures higher than T_b , all AFM spins reverse during the magnetization loop of the FM. While the FM spins are switched by the external magnetic field, they drag the AFM spins irreversibly, hence increasing the coercivity. For pinning of some fraction of AFM spins at lower temperatures (below T_b), the FM does not drag all of the AFM spins, consequently the exchange bias effect occurs, and H_C is reduced. This results in a peak

in H_C at around T_b . For thinner NiMn layers, no stable pinning of AFM spins occurs in the studied temperature range to “freeze” the AFM spins against being dragged by the FM magnetization. Therefore no EB can be observed.

V. SUMMARY

Thickness-dependent H_C of polar MOKE measurements on OoP magnetized NiMn/9.3 ML Ni/Cu₃Au(001) showed that ~ 7 ML of equi-atomic single-crystalline NiMn order antiferromagnetically at room temperature. It is further observed that NiMn thin films as an AFM material can couple to both OoP as well as IP magnetized ferromagnetic Ni films. The finite-size effect of T_{AFM} for NiMn is observed both in IP and OoP cases. The ordering temperature of NiMn is much higher when coupled to Ni magnetized in OoP than in IP direction. This shift of ordering temperature (as high as 110 K), while switching the interfacial coupling from perpendicular to in-plane by manipulating the Ni magnetization direction, is the result of a magnetic proximity effect which in turn is either due to (i) the different interface coupling strength and/or (ii) the NiMn spin structure, which is deviated in such a way that it is thermally more stable when coupled to OoP Ni compared to IP Ni. An exchange-bias effect is only observed for the thickest NiMn film studied, where slightly higher T_b and H_{eb} values for OoP samples than for IP ones are observed and attributed to the influence of T_{AFM} . On the basis of our findings, it can be concluded that the spin structure of equi-atomic NiMn thin film alloys epitaxially grown on Ni/(Co)/Cu₃Au(001) is either non-collinear, at variance from its collinear bulk spin structure,^{14,15} or that the NiMn spins follow the spin orientation of the adjacent Ni layer under the respective field cooling directions.

ACKNOWLEDGMENTS

M.Y.K. is grateful for financial support during his stay in Berlin by the Higher Education Commission (HEC) of Pakistan through Kohat University of Science and Technology (KUST), Kohat, Pakistan and Freie Universität Berlin. M.E. would like to thank The Council of Higher Education (Turkey) for the financial support during his stay in Berlin. We acknowledge the technical assistance of M. Bernien.

¹S. A. Wolf, D. D. Awschalom, R. A. Buhrman, J. M. Daughton, S. von Molnár, M. L. Roukes, A. Y. Chtchelkanova, and D. M. Treger, *Science* **294**, 1488 (2001).

²W. H. Meiklejohn and C. P. Bean, *Phys. Rev.* **102**, 1413 (1956).

³G. A. Prinz, *Science* **282**, 1660 (1998).

⁴S. S. P. Parkin, K. P. Roche, M. G. Samant, P. M. Rice, and R. B. Beyers, R. E. Scheuerlein, E. J. O’Sullivan, S. L. Brown, J. Bucchignano, D. W. Abraham, Y. Lu, M. Rooks, P. L. Trouilloud, R. A. Wanner, and W. J. Gallagher, *J. Appl. Phys.* **85**, 5828 (1999).

⁵J. Nogués and I. K. Schuller, *J. Magn. Magn. Mater.* **192**, 203 (1999).

⁶Y. Wu, “Nano spintronics for data storage,” in *Encyclopedia for Nanoscience and Nanotechnology*, edited by H. S. Nalwa (American Scientific, Valencia, CA, 2003), Vol. 7, p. 493.

⁷E. Krén, E. Nagy, I. Nagy, L. Pál, and P. Szabó, *J. Phys. Chem. Solids* **29**, 101 (1968).

⁸B. Dai, J. W. Cai, W. Y. Lai, F. Shen, Z. Zhang, and G. H. Yu, *Appl. Phys. Lett.* **82**, 3722 (2003).

- ⁹W. A. A. Macedo, P. L. Gastelois, M. D. Martins, W. Kuch, J. Miguel, and M. Y. Khan, *Phys. Rev. B* **82**, 134423 (2010).
- ¹⁰K. Lenz, S. Zander, and W. Kuch, *Phys. Rev. Lett.* **98**, 237201 (2007).
- ¹¹J. Wang, W. Kuch, L. I. Chelaru, F. Offi, and M. Kotsugi, *Appl. Phys. Lett.* **86**, 122504 (2005).
- ¹²W. Kuch, L. I. Chelaru, F. Offi, J. Wang, M. Kotsugi, and J. Kirschner, *Phys. Rev. Lett.* **92**, 017201(2004).
- ¹³C. H. Marrows, *Phys. Rev. B* **68**, 012405 (2003).
- ¹⁴J. S. Kasper and J. S. Kouvel, *J. Phys. Chem. Solids* **11**, 231 (1959).
- ¹⁵L. Pál, E. Krén, G. Kádár, P. Szabó, and T. Tarnóczy, *J. Appl. Phys.* **39**, 538 (1968).
- ¹⁶D. Spišák and J. Hafner, *J. Phys. Condens. Matter* **11**, 6359 (1999).
- ¹⁷A. Sakuma, *J. Magn. Magn. Mater.* **187**, 105 (1998).
- ¹⁸M. S. Lund, M. R. Fitzsimmons, S. Park, and C. Leighton, *Appl. Phys. Lett.* **85**, 2845 (2004).
- ¹⁹C. Tieg, W. Kuch, S. G. Wang, and J. Kirschner, *Phys. Rev. B* **74**, 094420 (2006).
- ²⁰M. Reinhardt, J. Seifert, M. Busch, and H. Winter, *Phys. Rev. B* **81**, 134433 (2010).
- ²¹C. L. Gao, A. Ernst, A. Winkelmann, J. Henk, W. Wulfhekel, P. Bruno, and J. Kirschner, *Phys. Rev. Lett.* **100**, 237203 (2008).
- ²²M. Stampe, P. Stoll, T. Homberg, K. Lenz, and W. Kuch, *Phys. Rev. B* **81**, 104420 (2010).
- ²³F. Offi, W. Kuch, and J. Kirschner, *Phys. Rev. B* **66**, 064419 (2002).
- ²⁴M. Ali, P. Adie, C. H. Marrows, D. Greig, B. J. Hickey, and R. L. Stamps, *Nature Mater.* **6**, 70(2007).
- ²⁵M. Ali, C. H. Marrows, M. Al-Jawad, B. J. Hickey, A. Misra, U. Nowak, and K. D. Usadel, *Phys. Rev. B* **68**, 214420 (2003).
- ²⁶H. C. N. Tolentino, M. D. Santis, J. M. Tonnerre, A. Y. Ramos, V. Langlais, S. Grenier, and A. Bailly, *Braz. J. Phys.* **39**, 150 (2009).
- ²⁷W. Pan, N. Y. Jih, C. C. Kuo, and M. T. Lin, *J. Appl. Phys.* **95**, 7297 (2004).
- ²⁸W. Kuch, L. I. Chelaru, F. Offi, J. Wang, M. Kotsugi, and J. Kirschner, *Nature Mater.* **5**, 128 (2006).